Journal of Environmental Chemical Engineering 1 (2013) 838–843

Contents lists available at ScienceDirect

Journal of Environmental Chemical Engineering

journal homepage: www.elsevier.com/locate/jece

Efficient adsorption and desorption of Pb^{2+} from aqueous solution

Zhen Zhu, Wei Li *

Key Laboratory of Advanced Energy Materials Chemistry (Ministry of Education), College of Chemistry, Nankai University, Tianjin, 300071, China

ARTICLE INFO

Article history:
Received 22 February 2013
Accepted 22 July 2013

Keywords:
Functionalized
Adsorption
Pb^{2+}
Regeneration

ABSTRACT

Zinc oxide-functionalized MCM-41 (ZM) was used for the removal of Pb^{2+} from aqueous solution, and variables of the system were studied. The experimental data were correlated with the Langmuir isotherm model. The maximum adsorption capacity of ZM for Pb^{2+} was found to be 549.87 mg/g at room temperature and the adsorption capacity was able to remove sufficient Pb^{2+} to achieve drinking water standards (<10 ng/mL). The thermodynamic parameters such as changes in free energy (ΔG), enthalpy (ΔH), and entropy (ΔS) were derived to indicating that the adsorption process to be endothermic in nature. The efficiency of ZM for adsorption of Pb^{2+} did not change significantly and a maximum 1% decrease was observed after 10 cycles, meeting the safe regulatory discharge standard (<100 ng/mL). Moreover, a novel freezing regeneration method was developed that could reduce the cost of desorption and prolong the life of the adsorbent. Therefore, the adsorbent ZM has potential as a promising application in the field of water pollution control.

Introduction

Heavy metal contamination of water poses a serious threat to the global ecosystem. Strict environmental protection legislation and public environmental concerns are driving the search for new amelioration techniques [1]. Among the known heavy metal ions, Pb^{2+} is one of the most dangerous, causing adverse health effects from lead exposure, particularly in children. Various symptoms have been attributed to lead poisoning, including abdominal pain and vomiting. The accumulation of Pb^{2+} in the human body can introduce a range of serious health afflictions, including muscle paralysis, mental confusion, memory loss, and anemia, suggesting that Pb^{2+} affects multiple targets in vivo [2]. Even worse is that such pollution may persist for two millennia [3]. Due to its high toxicity, a lot of effort has been expended on developing techniques to effectively remove Pb^{2+} from water. Several methods, such as biological treatment, membrane processes, ion exchange, ultrafiltration, solvent extraction, chemical precipitation, phytoextraction and adsorption procedures are the common methods of removing Pb^{2+} from aqueous solutions [4–19]. Among these approaches, the adsorption method seems as one of the most prominent choice because of its low cost and minimized amount of Pb^{2+}. The adsorption process has received much attention, especially for wastewater that contains low concentrations of metals and complex-forming substances. MCM-41 (a hexagonal (space group *p*6*mm*) material), which has a high surface area, should provide an efficient surface for the functional groups. Therefore, MCM-41 could be the ideal support for designing general purpose adsorbents. At the same time, the functional groups, such as EDTA [20], 5-mercapto-1-methyl-1-*H*-tetrazol [21], tetraborate [22] and metal oxide [23], can improve the heavy metal adsorption capacity of mesoporous silica.

So far there has been no report in the literature about the interaction between Pb^{2+} and zinc oxide-functionalized MCM-41 (denoted as ZM). The aim of this paper is to examine the effectiveness of the adsorbent ZM in removing Pb^{2+} from aqueous solution and to determine the adsorption characteristics of Pb^{2+} onto ZM. Compared with the acid regeneration method [24–26], we designed a new regeneration method, regeneration by washing with deionized water instead of traditional desorption agents, such as hydrochloric acid.

Experimental

Materials

All the reagents used in this study were analytical grade and were used as purchased without further purification. Mesoporous MCM-41 was purchased from Tianjin Chemist Technology Development Ltd., China. Zinc nitrate ($Zn(NO_3)_2$), lead nitrate ($Pb(NO_3)_2$) and hydrochloric acid (HCl) were purchased from Tianjin Jiangtian Chemical Technology Ltd., China. Home-made ZnO was prepared by calcined in air at 673 K for 3 h.

* Corresponding author. Tel.: +86 22 23508662; fax: +86 22 23508662.
E-mail address: weili@nankai.edu.cn (W. Li).

2213-3437/$ – see front matter © 2013 Elsevier Ltd. All rights reserved.
http://dx.doi.org/10.1016/j.jece.2013.07.022

Synthesis of adsorbents

Zinc nitrate was dissolved in deionized water to prepare the solution. The solution was mixed with MCM-41, and the mixture was agitated at room temperature (298 K) for 1 h to impregnate MCM-41 with the metal ions. The MCM-41 was then filtered and cleaned using deionized water, dried in an oven for 3 h at 373 K, and calcined in air at 673 K for 3 h. The functionalized MCM-41 is referred to as ZM.

Characterization

Powder X-ray diffraction spectra were collected using a Bruker D8 focus diffractometer, with Cu Kα radiation at 40 kV and 40 mA. Nitrogen adsorption–desorption isotherms of samples at 77 K were measured using a BEL-MINI adsorption analyzer. The surface area was calculated using a multipoint Brunauer–Emmett–Teller (BET) model. The total pore volume was estimated at a relative pressure of 0.99, assuming full surface saturation by nitrogen. The amount of zinc oxide was measured by using an AAS (TAS-990), after ZM was dissolved into 1 M hydrochloric acid solution. Infrared spectra were measured on a Nicolet Nexus 870, Fourier transform spectrometer in the frequency range 400–4000 cm^{-1}. Samples were pulverized and dispersed in KBr pellets before recording the spectra.

Batch adsorption experiments

The experiments were performed in a temperature-controlled water bath shaker for a certain time at a mixing speed of 180 rpm. The effects of contact time, pH and temperature on adsorption data were assessed by changing the adsorption conditions. The stock solution of Pb^{2+} was prepared by dissolving lead nitrate ($Pb(NO_3)_2$) in deionized water. Batch adsorption experiments were conducted using 0.05 g of adsorbent with 25 mL of solutions containing Pb^{2+} at the desired concentration (adsorbent dose = 2 g/L). The initial concentration varied from 10 to 2000 mg/L. The initial pH of the solution was adjusted with 1 M HCl solution and 1 M NaOH solution to reach a desirable value (pH 1–13). On completion of the adsorption process, the solutions were filtered and the residual concentration of Pb^{2+} was determined using the AAS (TAS-990). The percentage removal of Pb^{2+} was calculated according to the following equation:

$$R = \frac{C_0 - C_e}{C_0} \times 100\% \quad (1)$$

The adsorption amount (Q_e) was calculated according to the following equation:

$$Q_e = \frac{V(C_0 - C_e)}{m} \quad (2)$$

where Q_e is the amount (mg/g) of metal ions adsorbed by the ZM, C_0 and C_e are the metal concentrations (mg/L) in the solution initially and after adsorption, respectively, V is the volume (L) of the solution, and m is the mass (g) of adsorbent used in the experiments.

Results and discussion

Characterization of the adsorbents

The typical diffraction peaks of zinc oxide (the peaks at $2\theta = 31.69°$, 34.36°, 36.18°, 47.54°, 56.51°, 62.78°, 66.30°, 67.96°, 69.10°) are clearly visible in Fig. 1b. All peaks of the sample are close to the values reported in the Joint Committee on Powder Diffraction Standards (JCPDS) card no. 36-1451, which indicates the formation of zinc oxide. It is worth noting that zinc oxide groups have functionalized onto the surface of MCM-41. Meanwhile, the small-angle X-ray diffraction (XRD) patterns for MCM-41 and ZM samples are shown in Fig. 1a. Hexagonally arranged channels, represented by (100), (110), and (200) reflections existed in the samples. The reflection intensity decreased after functionalization, showing that abundant functional groups have occupied the surface of MCM-41, and the porous channels remained in a hexagonal array. We also found that the BET surface area and total pore volume decreased from 834 to 451 $m^2\,g^{-1}$ and from 0.92 to 0.68 $cm^3\,g^{-1}$, respectively, after functionalization. ZnO groups might have reduced the silica gel pore volume. This result shows that functional groups were successfully loaded onto the MCM-41 surface with pendant groups present on the silica surface partially blocking the adsorption of nitrogen molecules.

Effect of pH values on Pb^{2+} adsorption

The adsorption of Pb^{2+} was highly dependent on the initial pH of heavy metal ions solution because the pH affects the adsorbent surface charge, the degree of ionization and the variety of adsorbate. The adsorption experiments were conducted in the initial pH range of 1–13. Pb^{2+} precipitate as insoluble hydroxides because of the high concentration of OH^- ions in the aqueous solution [27,28]. As illustrated in Fig. 2, it was found that the adsorption capacity for Pb^{2+} was minimal at low pH. This was because, at low pH, the concentration of H^+ ions far exceeds that of the metal ions and hence H^+ ions react with zinc oxide, causing the amount of zinc oxide to decrease ($ZnO + 2H^+ = Zn^{2+} + H_2O$). However, as the pH increases, the adsorption capacity is also increased as the corrosive effect of acidic solution is reduced. At higher pH values, precipitation of metal hydroxides may account for metal removal. There would then be a decrease in the abundance of positive surface active sites, which would lower the electrostatic repulsion between the positively charged Pb^{2+}

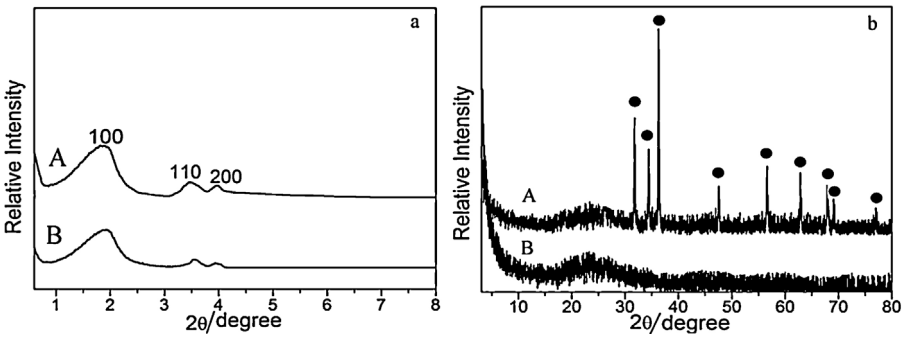

Fig. 1. (a) The small angle XRD patterns of MCM-41 and ZM; (b) the XRD patterns of MCM-41 and ZM ((a) A: MCM-41; B: ZM; (b) A: ZM, ●, the typical diffraction peaks of ZnO; B: MCM-41).

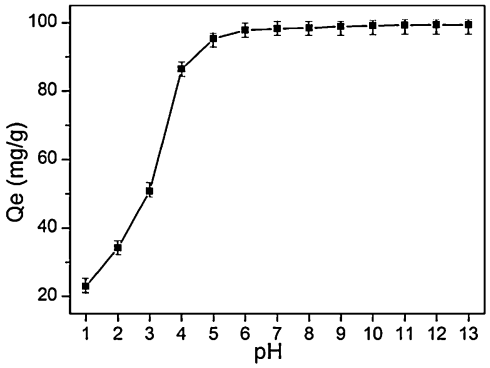

Fig. 2. Plot of % Pb^{2+} removal against pH on ZM (adsorption conditions: initial Pb^{2+} concentration = 200 mg/L, adsorbent dose = 2 g/L, contact time = 120 min, temperature = 298 K, pH = 1–13).

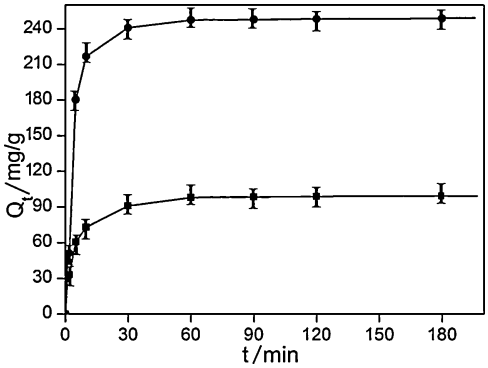

Fig. 4. Plot of Pb^{2+} adsorption capacity Qt against contact time on ZM (adsorption conditions initial Pb^{2+} concentration = (200 and 500) mg/L, adsorbent dose = 2 g/L, pH = 7, temperature = 298 K, contact time = 120 min (■, initial Pb^{2+} concentration = 200 mg/L; ●, initial Pb^{2+} concentration = 500 mg/L).

and the surface of the ZM. This would increase the Pb^{2+}-binding capacity. Under neutral condition, ZM displayed excellent Pb^{2+} adsorption efficiency. Thus, a pH value of 7 was used as the optimum pH value throughout the tests.

Adsorption performance of different adsorbents

As shown in Fig. 3a, the Pb^{2+} adsorption capacity increased gradually with increased mole, and reached peak capacity at 25 wt% loading corresponding to 119.5 mg/g. This value is five times that for MCM-41. This clearly shows that MCM-41 has a synergistic effect on the adsorption of Pb^{2+} when ZnO is loaded into its porous structure. The synergistic effect of the MCM-41 is related to the pore structure of the adsorbent with different zinc oxide loadings. A suitable loading of zinc oxides is vital for Pb^{2+} adsorption capacity. We also found that ZM reinforced the Pb^{2+} adsorption capacity through a cooperative effect related to the pores in the MCM-41, as shown in Fig. 3b.

These results prove that ZnO groups in the adsorbent are effective adsorption sites and that increasing the number of functional groups increases the Pb^{2+} adsorption capacity of functionalized MCM-41. The OH^- ion was supplied from dissociation of $Zn(OH)_2$ formed on the surface of ZnO particles, which would be the same reaction in the case of home-made ZnO. High pH (OH^- concentration) in the region near the material surface gives favorable conditions for Pb^{2+} to precipitate on the surface as hydroxide even if the pH of the bulk solution is lower than that at which $Pb(OH)_2$ starts to precipitate (calculated from the K_{sp} of $Pb(OH)_2$). Zinc oxide is thus loaded onto MCM-41 to increase its capacity to absorb Pb^{2+} ions, by creating hydroxyl groups on zinc oxide in aqueous solution. There are two possible reasons for the synergistic effect of the ZM: The uniform mesoporous channels of MCM-41 may play an important role in the increase in the Pb^{2+} adsorption capacity. When these channels are filled with zinc oxide, the pore volume of MCM-41 decreases. At the same time, more Pb^{2+} affinity sites are introduced into the channel. These two effects may combine and result in a further increment in adsorption capacity. Although dispersion of zinc oxide on material with a high surface area can increase the adsorption capacity, it is the "molecular basket" concept that causes the large increase in capacity. ZnO groups in pores have more accessibility to Pb^{2+}, so precipitation of $Pb(OH)_2$ is more likely to occur in the region near an MCM-41 surface than in the bulk solution, and the precipitated $Pb(OH)_2$ is more strongly retained on the surface compared with the presence of zinc oxide alone. In addition, the adsorption capacity of ZM increased until the loading of zinc oxide reached 25 wt%.

Effect of contact time on Pb^{2+} adsorption

The effect of shaking time was studied using a constant concentration of Pb^{2+} solution at $T = 298$ K and adsorbent dose = 2 g/L. The sorption of Pb^{2+} has been investigated onto ZM as a function of time in the range of (5–200) min. The amount of Pb^{2+} adsorbed by the ZM was determined with initial concentrations of 200 mg/L and 500 mg/L, respectively. As illustrated in Fig. 4, the apparent adsorption equilibrium was usually established within 60 min and no significant change in the amount of Pb^{2+} adsorbed was observed after 120 min. This was because of the high complexation rate between Pb^{2+} and reactive functional groups on the surface of ZM.

Adsorption isotherms

The adsorption isotherms of Pb^{2+} on ZM were studied at 273, 298, and 323 K to investigate the effect of temperature (adsorbent

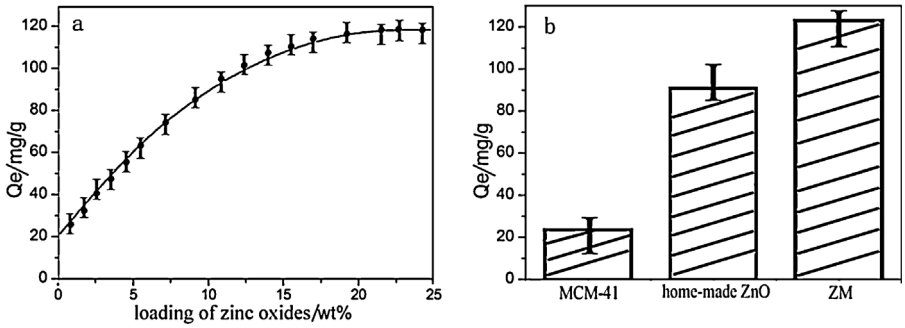

Fig. 3. (a) Plot of Pb^{2+} adsorption amount at different concentration of functional group; (b) adsorption capacity of different adsorbents for Pb^{2+} ((a) adsorption conditions: initial Pb^{2+} concentration = 250 mg/L, adsorbent dose = 2 g/L, contact time = 120 min, pH = 7, temperature = 298 K).

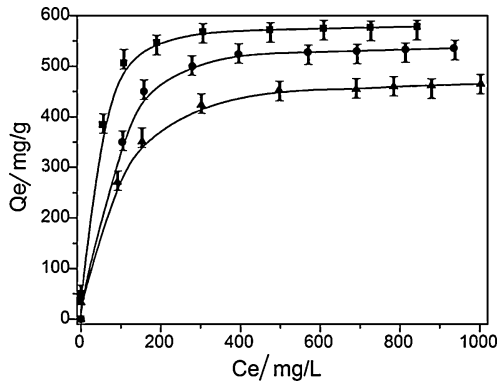

Fig. 5. Plot of Pb^{2+} amount adsorbed against different temperatures on ZM (adsorption conditions: adsorbent dose = 2 g/L, contact time = 120 min, pH = 7) (■, T = 323 K; ●, T = 298 K; ▲, T = 273 K).

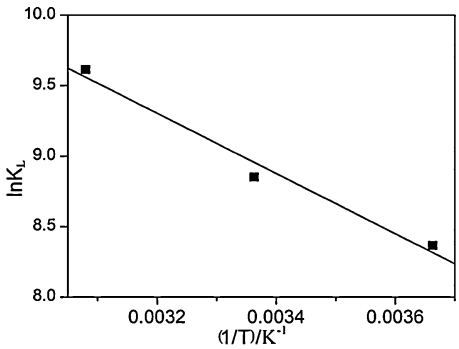

Fig. 6. Plot of ln K_L against reciprocal temperature.

dose = 2 g/L, and pH = 7). As shown in Fig. 5, for each adsorption isotherm, the adsorption capacity of Pb^{2+} exhibits a very steep increase with an increase in initial Pb^{2+} concentration. The results clearly indicate that high-energy adsorption sites favor strong adsorption at low equilibrium concentrations. In contrast, at higher initial Pb^{2+} concentration, the adsorption capacity decreased gradually with decreased in the number of the adsorption sites (Pb^{2+} bind the adsorption sites), indicating that the number of adsorption sites on the surface of the ZM actually limits the adsorption capacity.

Langmuir and Freundlich model equations were selected for use in this study. These models suggest different adsorption modes for adsorbate–adsorbent interactions. The Langmuir model supposes a monolayer adsorption with a homogeneous distribution of adsorption sites and energies, without interactions between the adsorbed molecules or ions. To optimize the design of an adsorption system to remove metal ions from effluents, it is important to establish the most appropriate correlation for the equilibrium curve. The Langmuir adsorption isotherm has been successfully applied to many aqueous solution pollutant adsorption processes. It is commonly represented as:

$$Q_e = \frac{Q_0 K_L C_e}{1 + K_L C_e} \quad (3)$$

where Q_e represents the equilibrium adsorption capacity of Pb^{2+} on the adsorbent (mg/g), C_e represents the equilibrium concentration in solution (mg/L), Q_0 represents the maximum monolayer capacity of adsorbent (mg/g), and K_L represents the Langmuir adsorption constant (L/mg) related to the free energy of adsorption. In the case of the Freundlich model, the energetic distribution of sites is heterogeneous because of the diversity of adsorption sites or the diverse nature of the metal ions adsorbed, be they free or hydrolyzed. The Freundlich model considers a multilayer adsorption pattern. The Freundlich isotherm is an empirical equation describing adsorption onto a heterogeneous surface and has differing affinities for adsorption. The common form is:

$$Q_e = K_F C_e^{1/n} \quad (4)$$

where K_F (mg/g (L/mg)$^{1/n}$) and $1/n$ represent the Freundlich constants corresponding to adsorption capacity and adsorption intensity, respectively. The Langmuir and Freundlich model parameters and linear regression correlations (K_L,Q_0, K_F and $1/n$) obtained from curve fitting are given in Table 1. It can be seen that the linear regression correlations using the Langmuir model were better than those for the Freundlich isotherm for Pb^{2+}, which indicate that Freundlich isotherm model does not well describe the adsorption processes of ZM for Pb^{2+}. In addition, the Q_0 values for the adsorption of Pb^{2+} on ZM calculated from the Langmuir model are close to the experimental data. These results indicate that the Langmuir model better describes Pb^{2+} adsorption on ZM than the Freundlich model, a monolayer coverage of Pb^{2+} is considered to have formed on the surface of ZM. The monolayer capacity Q_0 of Pb^{2+} on ZM at 273 K (487.48 mg/g), 298 K (549.87 mg/g) and 323 K (587.93 mg/g), respectively, was calculated based on the Langmuir isotherm (Fig. 6). It is also noted that the adsorption capacity decreased with increasing the initial Pb^{2+} concentration. The maximum adsorption capacity decreased with increasing temperature, indicating that the adsorption process is endothermic. One possible explanation for this positive enthalpy is that Pb^{2+} dissolves well in water, and the hydration sheath of Pb^{2+} has to be destroyed before its adsorption on ZM. This dehydration process needs energy, and it is favored at high temperature (Table 2). K_L is the Langmuir adsorption constant (L/mol); T (K) is the temperature; R (J mol^{-1} K^{-1}) the gas constant, Q_e is the equilibrium adsorbate concentration in the aqueous phase (mg/g); C_e is the equilibrium concentration in solution (mg/L); and ΔS, ΔH and ΔG are the changes in entropy, enthalpy and the Gibbs energy, respectively. The negative values of ΔG indicate the spontaneous nature of the reaction, while the positive values of ΔS reflect an increase in the randomness at the solid–solution interface during the adsorption process. The values of ΔH and ΔS were determined from Van't Hoff equation and Gibbs free energy equation, when measured under the same experimental conditions. A linear plot of ln K_L versus $1/T$ is obtained from the model as shown in Fig. 6.

Van't Hoff equation:

$$\ln\left(\frac{Q_e}{C_e}\right) = -\frac{\Delta H}{RT} + c \quad (5)$$

Table 1
Parameters of adsorption model at different temperatures (ZM).

Temperature (K)	Langmuir model			Freundlich model		
	Q_0(mg/g)	K_L(L/mg)	R^2	K_F (mg/g (L/mg)$^{1/n}$)	$1/n$	R^2
273	487.08 ± 1.2	0.021	0.995	17.812 ± 4.2	0.272	0.909
298	549.87 ± 1.7	0.040	0.996	18.956 ± 5.5	0.293	0.916
323	588.34 ± 1.4	0.069	0.997	23.035 ± 4.7	0.284	0.908

Table 2
Thermodynamic data for adsorption of Pb^{2+} on ZM.

T (K)	K_L (L/mol)	ΔH (kJ/mol)	ΔS (J mol^{-1} K^{-1})	ΔG (kJ/mol)
273	4,298	17.74 ± 0.3	134.51 ± 2.1	−18.98
298	8,290	17.74 ± 0.5	134.51 ± 2.7	−22.34
323	14,451	17.74 ± 0.6	134.51 ± 1.8	−25.71

Table 3
Comparison of adsorption capacity of ZM for Pb^{2+} with that of different adsorbents.

Adsorbent	Adsorption capacity (mg/g)	Reference
DETA–MCM-41	193.65	[29]
DMDDA-41A	85.28	[30]
Thiol-functionalized MCM-41	102.54	[31]
Chitosan	132.48	[32]
Peelings radius	170.01	[33]
P(AA-Na)-grafted cotton	507.52	[34]
Aminated resin	201.76	[35]
ZM	549.87	This study

Gibbs free energy equation:

$$\Delta G = -RT \ln K_L \quad (6)$$

$$\Delta G = \Delta H - T\Delta S \quad (7)$$

Table 3 presents a comparison of the adsorption capacity of ZM for Pb^{2+} with that of various adsorbents in literature. Based on this table, it can be concluded that ZM has important potential for the removal of Pb^{2+} from aqueous solution.

Regeneration

For potential practical application, it is important to examine the possibility of desorbing the Pb^{2+} adsorbed on ZM and reusing them. Regeneration of loaded Pb^{2+}-sorbent is a key factor in a water treatment process. We designed a new regeneration approach, termed the freezing regeneration method. This method operates as follows: the adsorbed Pb^{2+}-loaded samples were placed in deionized water, stirred for 3 h at 273 K and then the samples were dried and reused for the next adsorption run. It is worth noting that ZM regeneration via our freezing method is that for an initial concentration of Pb^{2+} is 10 mg/L, 99% of the adsorption capacity of recycled ZM can still be maintained and a residual concentration of Pb^{2+} under 100 ng/mL (regulatory safe discharge standards) can be obtained at the 10th cycle. The adsorption capacity of Pb^{2+} is sufficient to reduce the residual concentration of Pb^{2+} to drinking water standards, as indicated in Fig. 7. Compared with acid regeneration, our freezing method can cut the cost of desorption agents such as hydrochloric acid. Consequently, it can be concluded that ZM can be used to remove trace Pb^{2+} from aqueous solution to meet regulatory safe discharge standards.

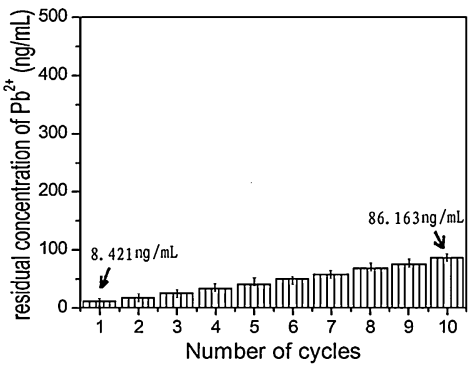

Fig. 7. Regenerated use of ZM for the removal of Pb^{2+} (adsorption conditions: initial Pb^{2+}concentration = 10 mg/L, adsorbent dose = 2 g/L, contact time = 120 min, pH = 7, temperature = 298 K) (1 mg/L = 1 μg/mol = 1000 ng/mL).

Conclusions

The adsorption of Pb^{2+} shows that the adsorption rate on ZM is very high and the adsorption isotherm fitted the Langmuir model well and the maximum adsorption capacity of ZM was 549.87 mg/g. The adsorption process was endothermic, favored at high temperature. The prominent adsorption capacity of ZM may be attributed to the zinc oxide. This causes a significant enhancement in the affinity for Pb^{2+}. The solution pH greatly influences the adsorption of Pb^{2+} from aqueous solution on ZM. Furthermore, the adsorption capacity of ZM for Pb^{2+} was superior compared with the ZnO particles because of its developed porous structure and high specific surface area. The adsorption capacity of Pb^{2+} was sufficient to reduce the residual concentration of Pb^{2+} to drinking water standards. It was also observed that the adsorption capacity for Pb^{2+} dropped slightly after each cycle. Regeneration of the Pb^{2+}-loaded adsorbent was achieved under mild conditions by washing with only deionized water without using desorption agents. The results indicate that the ZM can be recovered for consecutive use, thus ZM exhibited good reusability.

Acknowledgments

The authors acknowledge financial support from the National Natural Science Foundation of China (Grant no. 21073098), the Natural Science Foundation of Tianjin (11JCZDJC21600), and the Research Fund for 111 Project, the Doctoral Program of Higher Education (20090031110015), and the Program for New Century Excellent Talents in University (NCET-10-0481).

References

[1] R.M. Gong, Y. Ding, H.J. Liu, Q.Y. Chen, Z.L. Liu, Lead biosorption and desorption by intact and pretreated spirulina maxima biomass, Chemosphere 58 (2005) 125–130.
[2] H.Y. Lee, D.R. Bae, J.C. Park, H. Song, W.S. Han, J.H. Jung, A selective fluoroionophore based on BODIPY-functionalized magnetic silica nanoparticles: removal of Pb^{2+} from human blood, Angew. Chem. Int. Ed. 48 (2009) 1239–1243.
[3] S.M. Hong, J.P. Candelone, C.C. Patterson, C.F. Boutron, Greenland ice evidence of hemispheric lead pollution two millennia ago by Greek and Roman civilizations, Science 265 (1994) 1841–1843.
[4] A. Ahmad, R. Ghufran, W.M. Faizal, Cd(II), Pb(II) and Zn(II) removal from contaminated water by biosorption using activated sludge biomass, Clean-Soil Air Water 38 (2010) 153–158.
[5] H. Bessbousse, T. Rhlalou, J.F. Verchere, L. Lebrun, Removal of heavy metal ions from aqueous solutions by filtration with a novel complexing membrane containing poly(ethyleneimine) in a poly(vinyl alcohol) matrix, J. Membr. Sci. 307 (2008) 249–259.
[6] M.S. Berber-Mendoza, R. Leyva-Ramos, P. Alonso-Davila, L. Fuentes-Rubio, R.M. Guerrero-Coronado, Comparison of isotherms for the ion exchange of Pb(II) from aqueous solution onto homoionic clinoptilolite, J. Colloid Interface Sci. 301 (2006) 40–45.
[7] M.A. Farajzadeh, A.B. Monji, Adsorption characteristics of wheat bran towards heavy metal cations, Sep. Purif. Technol. 38 (2004) 197–207.
[8] L.V.A. Gurgel, L.F. Gil, Adsorption of Cu(II), Cd(II) and Pb(II) from aqueous single metal solutions by succinylated twice-mercerized sugarcane bagasse functionalized with triethylenetetramine, Water Res. 43 (2009) 4479–4488.
[9] J. Konczyk, C. Kozlowski, W. Walkowiak, Lead(II) removal from aqueous solutions by solvent extraction with tetracarboxylresorcin[4] arene, Physicochem. Probl. Miner. Process. 49 (2013) 213–222.
[10] I. Korus, Removal of Pb(II) ions by means of polyelectrolyte enhanced ultrafiltration, Polimery 55 (2010) 135–138.
[11] L.A. Holmes, A. Turner, R.C. Thompson, Adsorption of trace metals to plastic resin pellets in the marine environment, Environ. Pollut. 160 (2012) 42–48.
[12] M.K. Mondal, Removal of Pb(II) from aqueous solution by adsorption using activated tea waste, Korean J. Chem. Eng. 27 (2010) 144–151.
[13] N. Meunier, P. Drogui, C. Montane, R. Hausler, J.F. Blais, G. Mercier, Heavy metals removal from acidic and saline soil leachate using either electrochemical coagulation or chemical precipitation, J. Environ. Eng.-ASCE 132 (2006) 545–554.

[14] U. Wingenfelder, B. Nowack, G. Furrer, R. Schulin, Adsorption of Pb and Cd by amine-modified zeolite, Water Res. 39 (2005) 3287–3297.
[15] A. Sari, M. Tuzen, Kinetic and equilibrium studies of biosorption of Pb(II) and Cd(II) from aqueous solution by macrofungus (Amanita rubescens) biomass, J. Hazard. Mater. 164 (2009) 1004–1011.
[16] B. Singha, S.K. Das, Removal of Pb(II) ions from aqueous solution and industrial effluent using natural biosorbents, Environ. Sci. Pollut. Res. 19 (2012) 2212–2226.
[17] V.K. Sinhal, A. Srivastava, V.P. Singh, EDTA and citric acid mediated phytoextraction of Zn, Cu, Pb and Cd through marigold (*Tagetes erecta*), J. Environ. Biol. 31 (2010) 255–259.
[18] U. Suryavanshi, S.R. Shukla, Adsorption of Pb^{2+} by alkali-treated *Citrus limetta* peels, Ind. Eng. Chem. Res. 49 (2010) 11682–11688.
[19] L.Y. Yurlova, A.P. Kryvoruchko, Removal of Pb(II) ions from contaminated water by polymer-supported ultrafiltration, Adsorpt. Sci. Technol. 22 (2004) 543–551.
[20] J. Huang, M. Ye, Y.Q. Qu, L.F. Chu, R. Chen, Q.Z. He, D.F. Xu, Pb(II) removal from aqueous media by EDTA-modified mesoporous silica SBA-15, J. Colloid Interface Sci. 385 (2012) 137–146.
[21] D. Pérez-Quintanilla, A. Sánchez, I. del Hierr, M. Fajardo, I. Sierra, Functionalized HMS mesoporous silica as solid phase extractant for Pb(II) prior to its determination by flame atomic absorption spectrometry, J. Sep. Sci. 30 (2007) 1556–1567.
[22] E.I. Unuabonah, K.O. Adebowale, B.I. Olu-Owolabi, L.Z. Yang, L.X. Kong, Adsorption of Pb(II) and Cd(II) from aqueous solutions onto sodium tetraborate-modified Kaolinite clay: equilibrium and thermodynamic studies, Hydrometallurgy 93 (2008) 1–9.
[23] W.H. Zou, R.P. Han, Z.Z. Chen, J.H. Zhang, J. Shi, Kinetic study of adsorption of Cu(II) and Pb(II) from aqueous solutions using manganese oxide coated zeolite in batch mode, Colloid Surface A 279 (2006) 238–246.
[24] K.G. Bhattacharyya, A. Sharma, Adsorption of Pb(II) from aqueous solution by *Azadirachta indica* (neem) leaf powder, J. Hazard. Mater. 113 (2004) 97–109.
[25] L. Xiong, C. Chen, Q. Chen, J.R. Ni, Adsorption of Pb(II) and Cd(II) from aqueous solutions using titanate nanotubes prepared via hydrothermal method, J. Hazard. Mater. 189 (2011) 741–748.
[26] X.W. Zhao, G. Zhang, Q. Jia, C.J. Zhao, W.H. Zhou, W.J. Li, Adsorption of Cu(II), Pb(II), Co(II), Ni(II), and Cd(II) from aqueous solution by poly (aryl ether ketone) containing pendant carboxyl groups (PEK-L): equilibrium, kinetics, and thermodynamics,, Chem. Eng. J. 171 (2011) 152–158.
[27] M. Khotimchenko, V. Kovalev, Y. Khotimchenko, Equilibrium studies of sorption of lead(II) ions by different pectin compounds, J. Hazard. Mater. 149 (3) (2007) 693–699.
[28] M. Amini, H. Younesi, N. Bahramifar, A.A.Z. Lorestani, F. Ghorbani, A. Daneshi, M. Sharifzadeh, Application of response surface methodology for optimization of lead biosorption in an aqueous solution by *Aspergillus niger*, J. Hazard. Mater. 154 (1–3) (2008) 694–702.
[29] A. Benhamou, M. Baudu, Z. Derriche, J.P. Basly, Aqueous heavy metals removal on amine functionalized Si-MCM-41 and Si-MCM-48, J. Hazard. Mater. 171 (2009) 1001–1008.
[30] S.A. Idris, C.M. Davidsona, C. McManamon, M.A. Morris, P. Anderson, L.T. Gibsona, Large pore diameter MCM-41 and its application for lead removal from aqueous media, J. Hazard. Mater. 185 (2011) 898–904.
[31] S.J. Wu, F.T. Li, R. Xu, S.H. Wei, G.T. Li, Synthesis of thiol-functionalized MCM-41 mesoporous silicas and its application in Cu(II), Pb(II), Ag(I), and Cr(III) removal, J. Nanopart. Res. 12 (2010) 2111–2124.
[32] A. Kamari, I.D. Pulford, J.S.J. Hargreaves, Binding of heavy metal contaminants onto chitosans—an evaluation for remediation of metal contaminated soil and water, J. Environ. Manage. 92 (2011) 2675–2682.
[33] L. Niu, S.B. Deng, G. Yu, J. Huang, Efficient removal of Cu(II), Pb(II), Cr(VI) and As(V) from aqueous solution using an aminated resin prepared by surface-initiated atom transfer radical polymerization, Chem. Eng. J. 165 (2010) 751–757.
[34] H. Yang, R. Xu, X. Xue, F. Li, G. Li, Hybrid surfactant-template mesoporous silica formed in ethanol and its application for heavy metal removal, J. Hazard. Mater. 152 (2008) 690–698.
[35] Y.Q. Zen, S.B. Deng, L. Niu, F.J. Xu, M.Y. Chain, G. Yu, Functionalized cotton via surface-initiated atom transfer radical polymerization for enhanced sorption of Cu(II) and Pb(II), J. Hazard. Mater. 192 (2011) 1401–1408.